Available online at www.sciencedirect.com
SCIENCE DIRECT
International Journal of Mass Spectrometry 246 (2005) 105–112
International Journal of Mass Spectrometry
www.elsevier.com/locate/ijms

Electron-impact dissociative ionisation of the CCl_4 molecule

Borja Sierra [a], Roberto Martínez [b], Carolina Redondo [a], Fernando Castaño [a,*]

[a] *Facultad de Ciencia y Tecnología, Departamento de Química Física, Universidad del País Vasco, Apdo. 644, 48080 Bilbao, Spain*
[b] *Facultad de Farmacia, Departamento de Química Física, Universidad del País Vasco, Paseo de la Universidad, 7. 01006 Vitoria, Spain*

Received 8 June 2005; received in revised form 6 August 2005; accepted 12 August 2005
Available online 26 September 2005

Abstract

Absolute partial and total ionisation cross-sections, nascent ions kinetic energy distributions and the appearance energies of the product ions has been measured for the product ions produced by electron-impact on the CCl_4 molecule, namely CCl_3^+, CCl_2^+, CCl^+, Cl_2^+, Cl^+, C^+ and CCl_3^{2+} ions. The experiments were conducted by crossing a pulsed beam of tuneable energy electrons up to 100 and 0.5 eV (full with at half maximum) energy spread with a supersonic beam of CCl_4 in buffer Ar within the active region of a time-of-flight mass spectrometer. The total ionisation cross-section profile was calculated by adding the partial ionisation cross-section profiles. Both total and partial ionisation cross-sections are compared with previously reported theoretical and experimental results, analysing agreements and discrepancies. Appearance energies are also reported and combined with the nascent kinetic energy distributions lead to the identification of the fragmentation pathways.

Keywords: Electron-impact; Dissociative ionisation; Ionisation cross-sections; CCl_4

1. Introduction

The CCl_4 molecule is a member of the chlorofluoromethanes family that has attained widespread interest in the last decades due to its many industrial applications and undesired presence in the upper atmosphere [1] where it reacts and destroys some beneficial species. In the industry it is employed as a reactive etching gas for silicon wafers in microelectronic device fabrication, microelectro-mechanical-systems (MEMS), mass characterization, cleaning surfaces by chemical vapour deposition (CVD) [2], propellants and low temperature plasmas. Debris of these applications and naturally created halomethanes are released into the atmosphere where they are hazardous pollutants with a large residence lifetime in the upper atmosphere and a markedly efficient contribution to the greenhouse effect (GWP 2000 [1,3]).

Halomethanes yield highly reactive neutral plasmas when the collision energies of the components attain a few hundred electron volt. The most interesting properties of these plasmas stem from their efficient energy transfer and the presence of very reactive species to transform gases and surfaces. Most plasmas require a balance between electrons, ions and neutrals and electron-impact is pivotal to initiate and later sustain the plasma itself. In consequence, the study of the electron-impact with molecules is of dominant interest to understand and model etching and industrial plasmas and, in some cases, to choose efficient methods to obliterate the parent molecule [4].

The high electron affinity of CCl_4 (2.12 eV) has attracted considerable interest as a case study to yield negative ions. Indeed, nascent Cl^- ion is produced at virtually zero energy and the electron attachment cross-section is much higher than those for other chlorofluoromethanes [2].

This work completes our electron-impact investigation on chlorofluoromethanes CF_4, $CClF_3$, CCl_2F_2, CCl_3F series from threshold to 100 eV [5,6] and joins to the experimental partial and total ionisation cross-section (ICS) studies reported so far for CCl_4 [7–9] with the aim of shedding light on the nature of their significant disagreements. It also reports the electron-impact total ICSs and compares them with other experimental and theoretical outcomes [5–8] already published. In addition, the kinetic energy distributions of the product ions from CCl_4 have been investigated and used to identify the dissociation channels of the specific ions. A plausible comparison of the channels

* Corresponding author. Tel.: +34 94 601 2533; fax: +34 94 601 3500.
E-mail address: f.castano@ehu.es (F. Castaño).

1387-3806/$ – see front matter © 2005 Elsevier B.V. All rights reserved.
doi:10.1016/j.ijms.2005.08.006

and the ions associated with the virtual orbitals of the parent molecule is also presented.

2. Experimental

Electron-impact partial ICSs and kinetic energy distributions (KEDs) were measured in a linear, double-focusing, time-of-flight mass spectrometer (TOF-MS; R.M. Jordan). A detailed account of the experimental set-up has been presented elsewhere [10,11] and thus, only a succinct description is given here. Mixtures of CCl_4 vapour in rare gas (Ar or Kr) at a stagnant pressure of over 1 bar were prepared and stored in a stainless steel cylinder and stirred with a rotating magnet for at least 3 h. The homogeneity of the mixture was critical to obtain reproducible partial ICS measurements. The gas mixture was further expanded through a 0.8 mm Ø nozzle into the stainless steel chamber of the TOF-MS at a working pressure $<10^{-4}$ Torr. The resulting supersonic molecular beam was collimated by a skimmer and crossed at right angle with a tuneable energy pulsed electron beam (0.5 eV FWHM and 1–10 μA electron intensity) in the ionisation region of the TOF.

Measurements of the electron-impact appearance energy (AE) of the product ions were conducted at low intensities (1 μA) in order to minimize double collisions and ion production from channels other than that of the electron-parent molecule. Following the 300 ns electron pulse, the ejected ions are extracted to the acceleration region by a negative voltage pulse (145 V/cm) applied to the extraction grid, and further accelerated with a second electric field (1430 V/cm), which directs the bunch of ions towards the 86.5 cm long drift tube of the TOF. There, the ions were mildly focused with a couple of orthogonal deflection plates followed by a free flight along the tube until they finally impinge on the microchannel plate (MCP) detector placed at the far end of the flying tube.

Partial ICSs for both the ions of interest and the calibration buffer gas were monitored simultaneously to circumvent the influence of the electron intensity fluctuations. Absolute Ar^+ (39.9 amu) and Kr^+ (83.8 amu) ICSs were taken from Rejoub et al. [12]. Critical pressures for the initial gas mixture of CCl_4 and reference were measured with a capacitance manometer with nominal accuracy of 1% (MKS 750B).

Errors stem mostly from pressure inaccuracies (2–3% for CCl_4/Ar, Kr mixtures), uncertainties of reference gases ICSs (3–5% for Ar^+ and Kr^+), the percentage of ions that fail to reach the detector, and the single ion counting efficiency of the MCP detector. As discussed below, apparent ionisation energy thresholds are significantly affected by the KE excess of the ion and hence, considered as an upper limit of the ionisation energy. It is commonly accepted that lighter ions, such as C^+ and Cl^+, are ejected from Coulomb explosions (see below) with high KE (and usually broad KED) and, hence, are hard to focus on the MCP detector. Nascent KEDs were computed from the TOF band profiles, according to the method discussed elsewhere [10,11,13] and related to thermal and non-thermal contributions [10]. The total ICS (counting) was calculated by the addition of the partial ICSs of all the ions observed [14].

3. Results and discussion

3.1. Kinetic energy distributions of the product ions

The electron-impact energy employed to yield the dissociative ionisation can be split into two parts, the proper dissociative energy and that channelled toward the fragments internal degrees of freedom. In the case of atomic ions the excess energy appears as kinetic energy. The kinetic energy distribution of the product ions has been derived from the width and shape of the TOF mass bands [10,11,13] and are depicted in Fig. 1. Distributions with a feature peaking at low energy, say ≈0.5 eV, are related with a thermal relaxation and those with a second maximum at higher energies, to a non-thermal relaxation. Fig. 1 also shows that the lighter the released ions (C^+ and Cl^+) the larger their kinetic energy. The behaviour follows a similar pattern to that found for other members of the chlorofluoromethanes family [15]. In contrast, heavier ions, such as CCl_3^+, CCl_2^+, Cl_2^+ have much narrower KEDs primarily associated to a thermal release from the parent ion. Medium size ions, like CCl^+, has an intermediate behaviour, with a thermal peak at low energy ≈0.5 eV and a broad second band at higher energies. At high electron-impact energies the contributions narrow down and split into one peak at very low energy and a second at ≈0.7 eV that dominates the distribution. The KED of the low mass Cl^+ ion has two neat contributions, with a noticeable increase of the high energy band (at ≈4 eV) with the electron-impact energy. The feature may be attributed to the production of Cl^+ through a new channel that opens at an energy close to 30 eV (cf. below), and increases in efficiency with the electron-impact energy. Low mass C^+ ion KED has two contributions, one thermal centred at ≈0.4 eV and another broader between 3 and 6 eV. Both increase with the electron-impact energy.

It is worth noting that the characteristic KEDs of the dissociative ionisation barely change with the electron-impact energies and have patterns similar to those of fluoromethane and chlorofluoromethane [10,11]. Consequently, all the dissociative ionisation channels are opened near the ionisation threshold energies. However, the KE profiles determined at higher electron-impact energies are more accurate and reliable because of the higher mass spectra intensity.

3.2. Absolute partial ionisation cross-sections

Ions created by electron-impact on CCl_4 are unambiguously identified in our experimental set-up because of the characteristic splitting of the peaks arising from the ^{35}Cl and ^{37}Cl isotopes. The parent CCl_4^+ ion is not observed, as expected from its low stability and fast dissociative ionisation [16]. The ions detected include CCl_n^+ ($n = 1$–3), Cl_2^+, atomic Cl^+ and C^+, and CCl_3^{2+} dication. CCl_2^{2+} ion is also detected, but its intensity is so low as to hamper any sensible ICS determinations.

Fig. 2 depicts the partial ICS profiles obtained for all the product ions originated in the electron-impact on CCl_4 as a function of the electron-impact energy. The results are plotted along those reported by Leiter et al. [8] and Lindsay et al. [9]. For convenience purposes and future use, the numerical partial

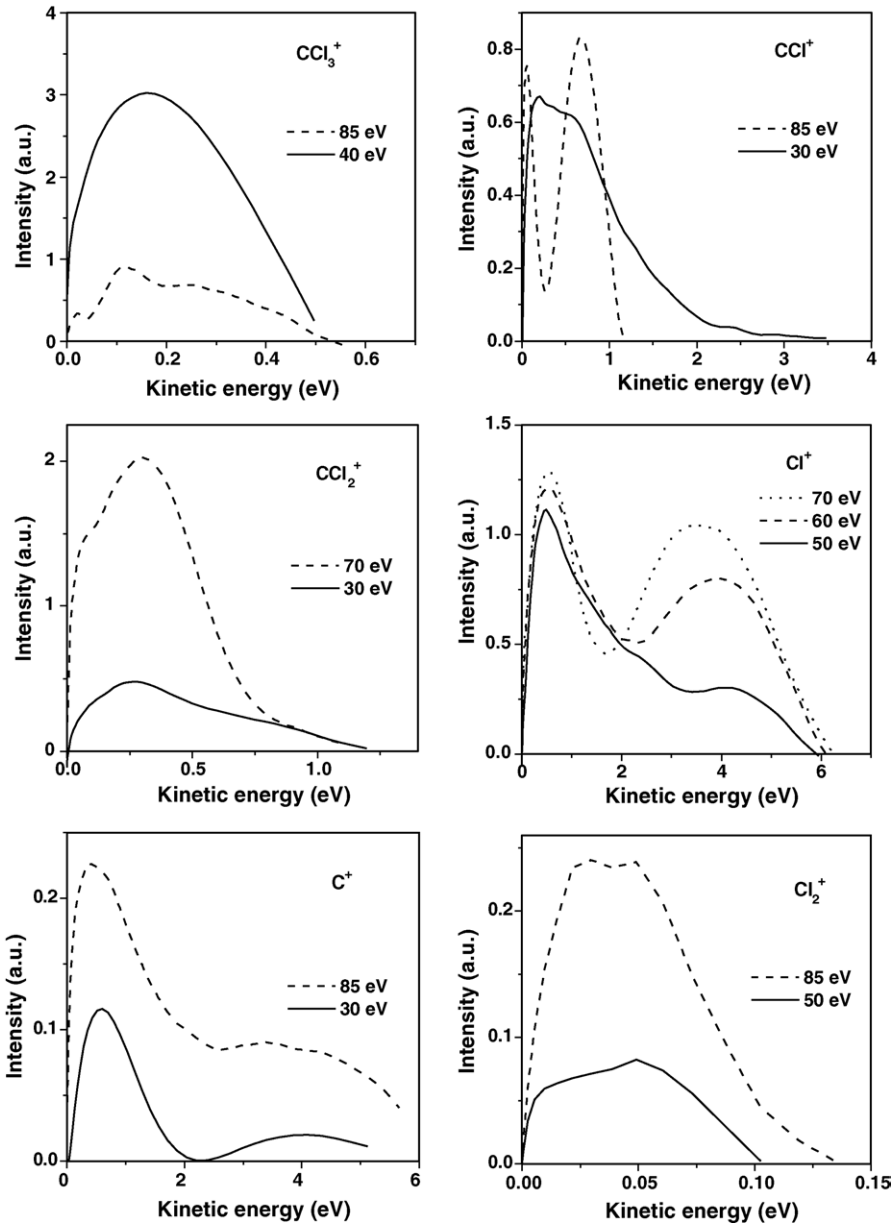

Fig. 1. KEDs of the set of ions produced by electron-impact on CCl_4. Note that the energy scales for the KEDs are different.

ICSs are also given in table form (Table 1). The last drawing of Fig. 2 shows the total ICS obtained by adding the partial ICSs of the ions at the selected impact energy, and compares it with the available experimental and theoretical results. In a previous paper [5], we presented the total ICS of the CCl_4 and compared it with those computed by the Deutsch and Märk formalism (DM), the modified additively rule (MAR), and a modified chlorine parametrised binary-encounter-Bethe (BEB) methods, with excellent agreement. The experimental total ICS profile obtained by the total ion current method [7] is also in good agreement with that presented in this work.

As expected, the ICSs of the product ions decrease in the series $CCl_3^+ > CCl^+ \approx CCl_2^+ > Cl^+$, a behaviour related with their stability. It should be noted that our partial ICS profiles are systematically and significantly higher than those of Leiter et al. [8]. The difference has, in some cases, an ICS ratio factor between two and three and cannot possibly be due to the loss of ions in the flight to the detector, but rather to a systematic error in the determination method, possibly in the measured CCl_4 absolute pressure. In fact, the CCl_4 vapour pressure at 23 °C is ca. 100 Torr and before the experiment the vapour ought to be mixed with Ar or Kr at a similar pressure to provide the internal reference ICS scale. At such low pressures, outgassing before and during storage and the gas dissolved in liquid CCl_4, and other causes lead to the presence of a non-negligible quantity of unwanted air in the mixing cylinder. To control the undesirable contamination, liquid CCl_4 must be freeze-pump-thawed a number of times, to be finally mixed with Ar under stirring conditions and for some hours. The presence of N_2^+ and O_2^+ ions in the mass spectra was used to estimate the presence of

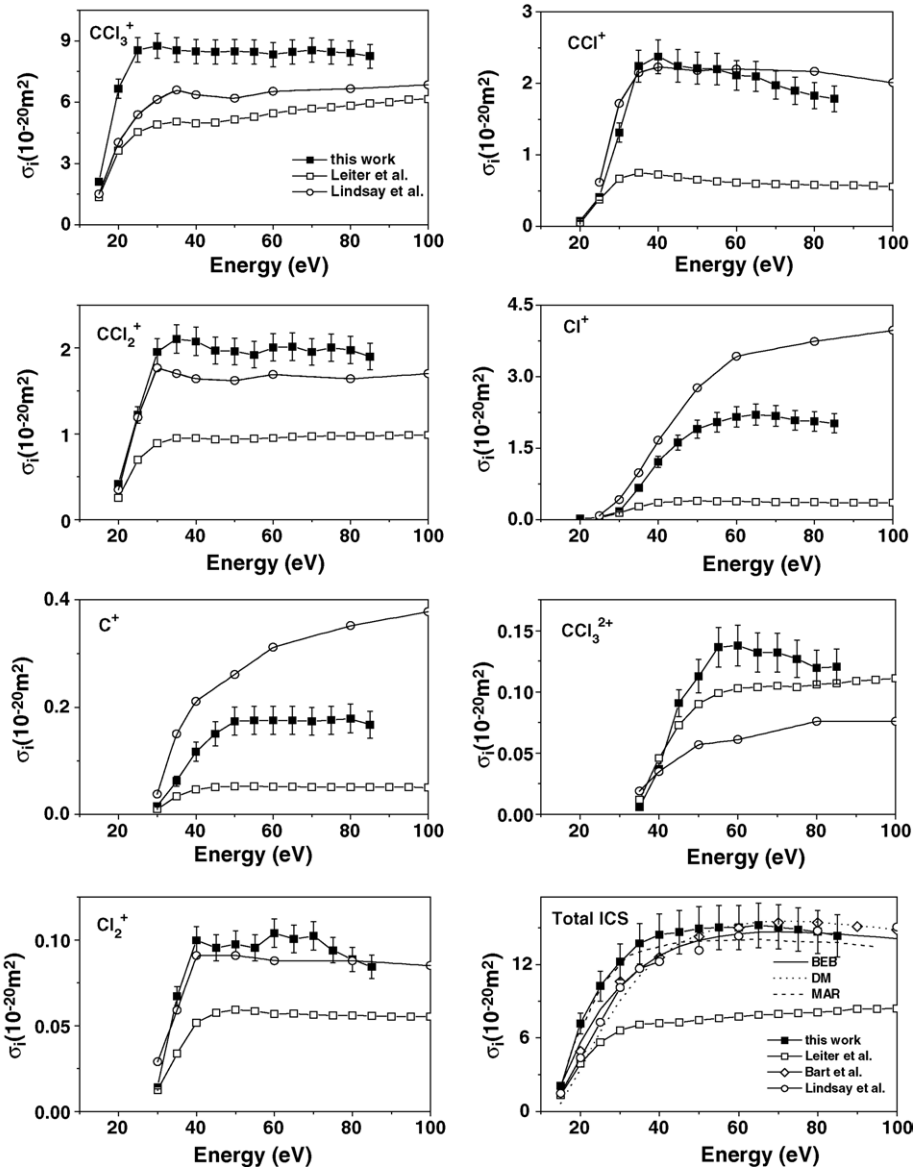

Fig. 2. Partial ionisation cross-section (ICS) profiles of the product ions of the electron-impact on the CCl_4 molecule, namely CCl_3^+, CCl^+, CCl_2^+, Cl^+, C^+, CCl_3^{2+}, Cl_2^+, as a function of the electron-impact energy. The very last plot at the bottom shows the total ICSs (computed as the sum of the partial ICSs) and contrasts the results with earlier reported experimental and computed values. (■) This work, (◊) Bart et al. [7], (□) Leiter et al. [8], (◯) Lindsay et al. [9], (—) modified chlorine parametrized binary-encounter-Bethe (BEB) method, Deutsch and Märk formalism (DM) and (- - - -) modified additively rule (MAR) approach.

air in the experiment and further to correct the CCl_4 absolute pressure.

A first glance at Fig. 2 shows that the C^+ and Cl^+ ions produced by Coulomb explosions have ICS profiles remarkably lower than those of Lindsay et al. [9] by a factor of 1.5 in contrast with heavy and low kinetic energy CCl_3^+, CCl_2^+ and CCl_3^{2+} ions where our ICSs are significantly superior by 40, 20 and 50%, respectively. The discrepancies may be attributed to the sensitivity of the experimental methods used to collect high kinetic energy ions. Lindsay et al. method is based [17] on the collision of an electron beam of monitored intensity with uniform density bulk gas target and collecting and determining the total number of ions extracted. The absolute partial ICSs are accomplished by the comparison of absolute electron and ion numbers, the density and the length travelled by the electrons in the sample. Our study obtains the ICSs by colliding two beams, one of electrons and another of a supersonic gas mixture including both the molecule investigated and the reference gas. The position-sensitive detector (PSD) of Lindsay is set close to the extraction grid, without tube-of-flight. Hence, the mass-resolution is very poor but, in contrast, ions released with high kinetic energy easily reach the detector and losses are minimized.

Two additional arguments must be considered to favour either the ICS data reported here and those by Lindsay et al. The finest theoretical methods provide a total ICS maximum of $15 \times 10^{-20}\,m^2$ at 60 eV, which differs from Leiter's profiles by a factor of two. Secondly, as discussed elsewhere [5], the CCl_4 molecule is expected to have higher total ICSs than chlorofluoromethanes with lower number of Cl atoms. In fact, the total ICSs of chlorofluoromethane follows the series $\sigma_{CF_4} <$

Table 1
Partial and total ionisation cross-sections of ions produced by electron-impact on CCl_4 (in 10^{-20} m^2 units)

Energy (eV)	CCl_3^+	CCl^+	CCl_2^+	Cl^+	C^+	CCl_3^{2+}	Cl_2^+	Total
15	2.10	–	–	–	–	–	–	2.10
20	6.66	0.08	0.41	0.02	–	–	–	7.18
25	8.55	0.41	1.22	0.05	–	–	–	10.23
30	8.75	1.32	1.96	0.17	0.02	–	0.01	12.22
35	8.55	2.24	2.11	0.66	0.06	0.01	0.07	13.70
40	8.49	2.38	2.08	1.21	0.12	0.04	0.10	14.41
45	8.46	2.25	1.97	1.61	0.15	0.09	0.10	14.63
50	8.47	2.21	1.96	1.90	0.17	0.11	0.10	14.93
55	8.45	2.20	1.92	2.04	0.18	0.14	0.09	15.03
60	8.33	2.11	2.01	2.16	0.18	0.14	0.10	15.03
65	8.46	2.10	2.01	2.20	0.18	0.13	0.10	15.19
70	8.54	1.98	1.96	2.18	0.17	0.13	0.10	15.07
75	8.47	1.89	2.00	2.08	0.17	0.13	0.09	14.84
80	8.40	1.83	1.98	2.06	0.18	0.12	0.09	14.66
85	8.24	1.79	1.90	2.02	0.17	0.12	0.08	14.33

$\sigma_{CClF_3} < \sigma_{CCl_2F_2} < \sigma_{CCl_3F} < \sigma_{CCl_4}$ whilst in Leiter's results [8] $\sigma_{CCl_4} < \sigma_{CCl_3F}$ and breaks the well established additivity rule [7] known to be followed in these processes.

3.3. Dissociative ionisation pathways

Electron-impact appearance energy thresholds are the upper limits of the channel dissociative ionisation energy because they includes the internal energy of the ejected fragments. Internal energies are usually far from easy to measure and in the case of atoms appear as kinetic energy. Fig. 3 collects the plots of the intensity profiles in arbitrary units versus the electron-impact energy for the ejected CCl_3^+, CCl^+, Cl_2^+ and CCl_3^{2+} ions. No reported measurements on the energy thresholds of the set of CCl_4 product ions have been reported so far, although Leiter et al. [8] mention the onset for the Cl_2^+ ion. Unfortunately, in their experiments the CCl_4 dissociates on the surface of the electron gun filament and the results are unreliable. The issue is circumvent in two colliding beam experiments. Some of the intensity/electron-impact energy profiles at threshold have a bent curved region, that prevents a straightforward and accurate determination [18], and raises the AE uncertainty.

Table 2 compares the ionisation channels and the experimental thresholds. The kinetic energies (column 4 in Table 2) are

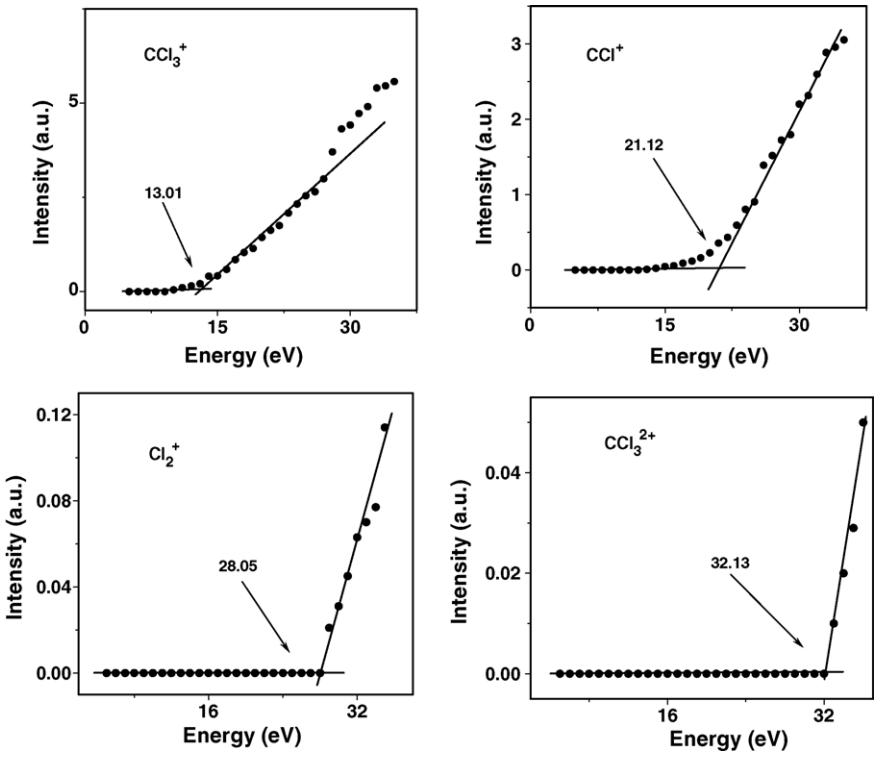

Fig. 3. Appearance energy (AE) of the CCl_3^+, CCl^+, Cl_2^+ and CCl_3^{2+} ions produced by electron-impact on CCl_4. Ar^+ ion was used to calibrate the electron energy scale (see text). A numerical list of the AEs for the ions is offered in Table 2.

Table 2
Correlation between the ionisation channels, referred to by a channel number, and the calculated and experimental thresholds for the most significant ion fragments produced by electron-impact on CCl_4

	Channel no.	ΔH° (eV)	Experimental threshold (other measurements)	Observed translational energy (eV)
1	$CCl_4 \rightarrow CCl_4^+$	11.32	Not observed	–
2	$CCl_4 \rightarrow CCl_3^+ + Cl$	10.98	13.01 ± 0.6	0–0.5
3	$CCl_4 \rightarrow CCl_3^+ + Cl^+$	24.02		
4	$CCl_4 \rightarrow CCl_2^+ + Cl_2$	12.65		
5	$CCl_4 \rightarrow CCl_2^+ + 2Cl$	15.17	18.03 ± 0.6	0–1.2
6	$CCl_4 \rightarrow CCl_2^+ + Cl + Cl^+$	28.20		
7	$CCl_4 \rightarrow CCl_2^+ + 2Cl^+$	41.24		
8	$CCl_4 \rightarrow CCl^+ + Cl_2 + Cl$	20.36	21.17 ± 0.8	0–0.3
9	$CCl_4 \rightarrow CCl^+ + 3Cl$	22.87		0.3–1.3
10	$CCl_4 \rightarrow CCl^+ + Cl_2^+ + Cl$	31.86		
11	$CCl_4 \rightarrow CCl^+ + Cl^+ + Cl_2$	33.39		
12	$CCl_4 \rightarrow CCl^+ + Cl^+ + 2Cl$	35.90		
13	$CCl_4 \rightarrow CCl_3^{2+} + Cl$	27.33	32.3 ± 1.0	
14	$CCl_4 \rightarrow CCl_3^{2+} + Cl^+$	40.36	$(30.4 \pm 0.3; 31.8 \pm 1.0; 33.1 \pm 0.3)$[a]	
15	$CCl_4 \rightarrow Cl_2^+ + CCl_2$	14.97		
16	$CCl_4 \rightarrow Cl_2^+ + CCl + Cl$	18.96		
17	$CCl_4 \rightarrow Cl_2^+ + C + Cl_2$	19.92		
18	$CCl_4 \rightarrow Cl_2^+ + C + 2Cl$	22.44	28.05 ± 1.0 (27.01)[a]	0–0.1
19	$CCl_4 \rightarrow Cl_2^+ + C^+ + Cl_2$	31.25		
20	$CCl_4 \rightarrow 2Cl_2^+ + C$	31.42		
21	$CCl_4 \rightarrow Cl_2^+ + C^+ + 2Cl$	33.76		
22	$CCl_4 \rightarrow C^+ + 2Cl_2$	19.75		
23	$CCl_4 \rightarrow C^+ + Cl_2 + 2Cl$	22.26		
24	$CCl_4 \rightarrow C^+ + 4Cl$	24.78	27.36 ± 1.0	0–2, 2.5–6
25	$CCl_4 \rightarrow C^+ + Cl_2^+ + Cl_2$	31.25		
26	$CCl_4 \rightarrow C^+ + Cl_2^+ + 2Cl$	33.76		
27	$CCl_4 \rightarrow Cl^+ + CCl_3$	16.11		
28	$CCl_4 \rightarrow Cl^+ + CCl_2 + Cl$	19.01		
29	$CCl_4 \rightarrow Cl^+ + Cl_2 + CCl$	20.49		
30	$CCl_4 \rightarrow Cl^+ + Cl_2 + Cl + C$	23.97}		
31	$CCl_4 \rightarrow Cl^+ + CCl_3^+$	24.02	26.09 ± 1.0	0–1.5, 2–6
32	$CCl_4 \rightarrow Cl^+ + 3Cl + C$	26.48		
33	$CCl_4 \rightarrow Cl^+ + CCl_2^+$	28.20		
34	$CCl_4 \rightarrow Cl^+ + Cl_2^+ + CCl$	31.99		
35	$CCl_4 \rightarrow Cl^+ + Cl_2 + CCl^+$	33.39		
36	$CCl_4 \rightarrow Cl^+ + Cl_2 + Cl + C^+$	35.29		

Only the energies closest to a determined channel are shown.
[a] Leiter et al. [8].

characteristic of the ionisation channel and must be subtracted in order to obtain the ionisation energy. AE thresholds were calculated from the enthalpies of formation [19–21] when available and otherwise computed by the Gaussian G2(MP3) method [22].

The outer occupied MOs of the CCl_4 molecule computed at the MP2/6-311G level are: $(1t_1)^6(3t_2)^6(1e)^4(2t_2)^6(2a_1)^2(1t_2)^6(1a_1)^2\ldots$ [5]. Bews and Glidewell [23] have reported a semiempirical MINDO/3 calculation suggesting the accessibility of a large number of excited states by electron-impact. For CCl_4^+ seven accessible bond states have been found from the low energy ionisation of CCl_4, but CCl_4^+ is separated by a low potential barrier, lower than the difference between the vertical and adiabatic energies of CCl_4, from fragment ions, such as CCl_3^+ or CCl_2^+. The calculations were confirmed by Deutsch et al. [16], who observed a low barrier between the CCl_4^+ states and the product ions.

Studies of PEPICO and TPEPICO photoelectron spectra suggest the presence of three bands at low ionisation energy [24]. All the ions formed in the low energy states dissociate into $CCl_3^+ + Cl$ fragments. At higher energies, the system associated with the dissociation may reach the C^2T_2 state, which dissociates into CCl_2^+ and CCl^+. Finally, Cl^+ formation is correlated with the D state.

Production of CCl_4^+ parent ion must be attained by extraction of electrons from $1t_1$ or $3t_2$ molecular orbitals, whose binding energies are 11.69 and 12.62 eV, respectively [5]. $1t_1$ or $3t_2$ orbitals are the lower energy states of the CCl_4 molecule and have a Cl lone-pair orbital character. The behaviour is similar to that of CF_4^+ ion [25], from which one expect that the withdrawal of one electron from the outer orbitals would have a small change

in the structure (if compared to the CCl_4 neutral molecule). Dissociation may be explained as an internal conversion to another electronic state. The appearance of CCl_4^+ and CF_4^+ ions [16] in metaestable states makes plausible the simplest model of the dissociation which considers that the lowest potential energy hypersurface of CCl_4^+ is repulsive in one direction but bound in others, particularly in those coordinates corresponding to the vibrations excited on ionisation.

According to the above discussion, CCl_3^+, CCl_2^+ and CCl^+ appearance energies match channels 2, 5 and 8, respectively (cf. Table 2), provided that the KED is low. 1e and $2t_2$ CCl_4 orbitals, have binding energies of 13.44 and 16.58 eV, respectively, and both have a C–Cl bonding character [5]. A simultaneous increasing of the electron-impact energy, withdrawal of electrons from the 1e and $2t_2$ orbitals and loss of the C–Cl bonding character justifies the bond breaking.

The CCl_3^{2+} dication appearance threshold has been determined to be 32.3 ± 1.0 eV, matching channel 13. AEs for this ion are difficult to measure, as implied by the dispersion of the reported thresholds [8]: 30.4 ± 0.3, 31.8 ± 1.0 and 33.1 ± 0.3 eV. Observation of dications is a significant matter since their instability and evolution to Coulomb explosions produce very high KE (see below) atoms and partner ions.

AE threshold of the thermal KE Cl_2^+ ion was determined to be 28.05 ± 1.0 eV. The onset is in agreement with the ≈27 eV (taken from Fig. 9 in reference [8]) from Leiter's. The closest dissociative channel, with a thermal KED, is 18, which also yields atomic fragments as partners. However, the energy difference between both experimental and theoretical AE is higher than the observed translational energy (5 eV versus 0–0.1 eV). In order to discuss this behaviour, we must consider other possibilities for dissociative ionisation channels driven to Cl_2^+. Fainelli et al. [26] studied the fragmentation of CCl_4 dications in an Auger electron-ion coincidence experiment. They estimated that a dissociative channel releasing Cl_2^+ is possible at 27.7 eV, as a result of the dissociation of the double ion configuration $(1t_1)^{-2}$. Unfortunately Cl_2^+ ion signals were too weak to make an intent to report the results.

Low mass C^+ and Cl^+ ions AE have been measured to be 27.36 ± 1.0 and 26.09 ± 1.0 eV, respectively. Both energies correlate well with channels 24 and 30–32, once compensated from the KE at threshold. The increase of the electron-impact energy, leads to a broadening and rising intensity of the band centred at ≈4 eV. The effect may be related to the yield of new dissociative channels. The broadened band appears at electron energy impact close to 30 eV, in good agreement with the $CCl_3^+Cl^+$ ion-pair formation. Evidence for $CCl_3^+Cl^+$ formation in stable states has been given by Grant et al. [27] who measured and calculated double ionisation energies for 12 singlet state of CCl_4^{2+}, starting at 29 ± 0.1 eV $(1t_1)^{-2}$, and for 14 triplet states beginning at 29.5 ± 0.2 eV $(1t_1)^{-2}$.

4. Conclusions

Nascent kinetic energy distribution, appearance energies and partial and total ionisation cross-sections are reported for all the observable ions produced by threshold to 100 eV electron-impact on the CCl_4 molecule. KED and AE provides enough background to identify the dissociative energy channels. ICSs are significantly different from those reported by Leiter et al. [8] and the agreement with Lindsay et al. partial ICSs [9] is not as satisfactory as expected.

Acknowledgements

The authors are grateful to MEC and MCYT (Madrid) for partial support of this work through Grants BQU2001-0511 and CTQ2004-07188/BQU; to GV (Vitoria) and to UPV for a Consolidated Research Group Grant (2001-05). B.S. thanks MEC (Madrid) for a graduate fellowship award.

References

[1] J.H. Seinfeld, S.N. Pandis, Atmospheric Chemistry and Physics. From Air Pollution to Climate Change, Wiley Inc., 1998.
[2] M. Konuma, Film Deposition by Plasma Techniques, Springer-Verlag, Berlin Heidelberg, 1992.
[3] E.C. Zipf, in: T.D. Märk, G.H. Dunn (Eds.), Electron Impact Ionisation, Springer-Verlag, Wien, 1985.
[4] S. Rubio, A. Rodero, M.C. Quintero, R. Alvarez, C. Lao, A. Gomero, ESCAMPIG16: 16th European Conference on Atomic and Molecular Physics of Ionized Gases, and ICRP5: 5th International Conference on Reactive Plasmas. Conference Proceedings, Grenoble (France), 2002.
[5] R. Martínez, B. Sierra, C. Redondo, M.N. Sánchez Rayo, F. Castaño, J. Chem. Phys. 121 (2004) 11653.
[6] I. Torres, R. Martínez, M.N. Sánchez Rayo, F. Castaño, J. Chem. Phys. 115 (2001) 4041.
[7] M. Bart, P.W. Harland, J.E. Hudson, C. Vallance, Phys. Chem. Chem. Phys. 3 (2001) 800.
[8] K. Leiter, K. Stephan, E. Märk, T.D. Märk, Plasma Chem. Plasma Process 4 (1984) 235, and references therein.
[9] B.G. Lindsay, K.F. McDonald, W.S. Yu, R.F. Stebbings, F.B. Yousif, J. Chem. Phys. 121 (2004) 1350.
[10] I. Torres, R. Martínez, M.N. Sánchez Rayo, F. Castaño, J. Phys. B: At. Mol. Opt. Phys. 33 (2000) 3615.
[11] B. Sierra, R. Martínez, F. Castaño, Int. J. Mass Spectrom. 225 (2003) 127.
[12] R. Rejoub, B.G. Lindsay, R.F. Stebbings, Phys. Rev. A 65 (2002) 042713.
[13] K. Schäfer, W.Y. Baek, K. Föster, D. Gassen, W. Neuwirth, Z. Phys. D 21 (1991) 137.
[14] B. Sierra, R. Martínez, C. Redondo, F. Castaño, Int. J. Mass Spectrom. 235 (2004) 223.
[15] B. Sierra, R. Martínez, F. Castaño, J. Phys. B: At. Mol. Opt. Phys. 37 (2004) 295.
[16] H. Deutsch, K. Leiter, T.D. Märk, Int. J. Mass Spectrom. Ion Proc. 67 (1985) 191.
[17] H.C. Straub, P. Renault, B.G. Lindsay, K.A. Smith, R.F. Stebbings, Phys. Rev. A 54 (1996) 2146.
[18] T.D. Märk, in: L.G. Christophorou (Ed.), Electron–Molecule Interactions and Their Applications, vol. I, Academic Press, Inc., 1984.
[19] JANAF, Thermochemical Tables, J. Phys. Chem. Ref. Data 14 (1985).
[20] K.P. Huber, G. Herzberg, Molecular Spectra and Molecular Structure. IV. Constants of Diatomic Molecules, Van Nostrand Reinhold, New York, 1979.
[21] L.G. Christophorou, J.K. Olthoff, J. Phys. Chem. Ref. Data 28 (1999) 131.
[22] L.A. Curtiss, K. Raghavachari, J.A. Pople, J. Chem. Phys. 98 (1997) 1293.
[23] J.R. Bews, C. Glidewell, J. Mol. Struct. 71 (1981) 287.

[24] T. Kinugawa, Y. Hikosaka, A.M. Hodgekins, J.H.D. Eland, J. Mass Spectrom. 37 (2002) 854.
[25] B. Brehm, R. Frey, A. Küstler, J.H.D. Eland, Int. J. Mass Spectrom. Ion Phys. 13 (1974) 251.
[26] E. Fainelli, F. Maracci, R. Platania, L. Avaldi, J. Electron Spectrosc. Relat. Phenom. 87 (1998) 169.
[27] R.P. Grant, F.M. Harris, S.R. Andrews, D.E. Parry, Int. J. Mass Spectrom. Ion Proc. 142 (1995) 117, and references therein.